IOPscience iopscience.iop.org

Home Search Collections Journals About Contact us My IOPscience

GaN-based magnetic semiconductors for nanospintronics

This article has been downloaded from IOPscience. Please scroll down to see the full text article.

2004 J. Phys.: Condens. Matter 16 S5555

(http://iopscience.iop.org/0953-8984/16/48/011)

View the table of contents for this issue, or go to the journal homepage for more

Download details:
IP Address: 129.252.86.83
The article was downloaded on 27/05/2010 at 19:17

Please note that terms and conditions apply.

INSTITUTE OF PHYSICS PUBLISHING JOURNAL OF PHYSICS: CONDENSED MATTER

J. Phys.: Condens. Matter **16** (2004) S5555–S5562 PII: S0953-8984(04)79452-7

GaN-based magnetic semiconductors for nanospintronics

H Asahi, Y K Zhou, M Hashimoto, M S Kim, X J Li, S Emura and S Hasegawa

The Institute of Scientific and Industrial Research, Osaka University, 8-1 Mihogaoka, Ibaraki, Osaka 567-0047, Japan

E-mail: asahi@sanken.osaka-u.ac.jp

Received 16 April 2004
Published 19 November 2004
Online at stacks.iop.org/JPhysCM/16/S5555
doi:10.1088/0953-8984/16/48/011

Abstract

GaN-based magnetic semiconductors are expected to exhibit ferromagnetism even at high temperatures. We have studied the magnetic and optical properties of transition-metal- and rare-earth-doped GaN. GaCrN showed ferromagnetic characteristics at 7–400 K. Clear hysteresis and clear saturation were observed in the magnetization versus magnetic field (M–H) curves at all measuring temperatures. We observed photoluminescence (PL) emission from GaCrN layers. GaGdN also showed ferromagnetic characteristics at 7–400 K. Sharp PL emission was observed for GaGdN. X-ray diffraction and EXAFS measurements showed no phase separation, and that the Cr and Gd atoms substitute Ga sites. Applications to novel devices controlling charges (electrons and holes), spins and photons are expected.

1. Introduction

III–V-based diluted magnetic semiconductors (DMSs) have been receiving great interest from the industrial viewpoint since the discovery of carrier-induced ferromagnetism in (In, Mn)As [1] and (Ga, Mn)As [2], because of their potential use as new functional materials that led to the introduction of spin degree-of-freedom into semiconductor devices. Magnetic semiconductors for practical applications require the following features. One is to have a Curie temperature (T_C) higher than room temperature, and the second is to be based on a typical semiconductor in which the carrier control technique is well established.

Recently, a theoretical study by first principles calculation was performed, and the possibility of magnetic semiconductors which show ferromagnetism at room temperature was reported [3]. Their calculation showed that V-, Mn- and Cr-doped GaN are promising candidates as room temperature ferromagnetic semiconductors and that Cr-doped GaN has the most stable ferromagnetic states. We have succeeded in the growth of GaCrN and

 © 2004 IOP Publishing Ltd Printed in the UK

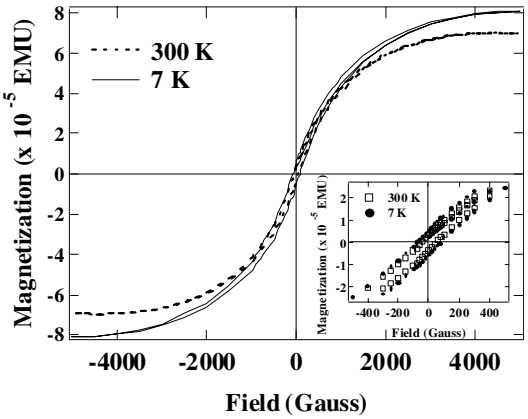

Figure 1. Dependence of magnetization on magnetic field at 7 and 300 K for GaCrN grown with Cr cell temperature of 850 °C. Clear saturation and hysteresis are observed at both temperatures.

observed ferromagnetic order at temperatures as high as 400 K [4]. Furthermore, we have observed photoluminescence (PL) emission from GaCrN [5]. We have also studied the magnetic properties of rare-earth-doped GaN, GaGdN and GaEuN, and observed ferromagnetic behaviour even at room temperature [6, 7].

In this paper, we will describe the experimental results on transition-metal-doped GaN and rare-earth-doped GaN.

2. GaCrN

GaCrN epitaxial layers were grown on sapphire (0001) substrates by MBE with an ion-removal electron–cyclotron-resonance (ECR) radical cell [4]. Elemental Ga, Cr and ECR plasma-enhanced N_2 were used as sources.

2.1. Structural properties

For the GaCrN sample grown with Cr cell temperature of 850 °C, x-ray diffraction rocking curves showed only diffraction peaks from hexagonal GaCrN (0002), (0004) as well as sapphire (0006), (0 0 0 12). No peaks from Cr–N or Cr–Ga compounds such as CrN, Cr_2N and $CrGa_4$ were observed. This clearly indicates that *c*-axis-oriented hexagonal GaCrN layers without any secondary phases were successfully obtained. The Cr concentration was estimated to be 1.5% for this sample. EXAFS measurement showed that the Cr atoms substituted the Ga sites. On the other hand, for the sample grown with Cr cell temperature of 940 °C, additional peaks were observed, indicating that phase separation occurs in this sample.

2.2. Magnetic properties

Figure 1 shows the magnetization versus magnetic field (M–H) curves at 7 and 300 K for the GaCrN sample grown with Cr cell temperature of 850 °C [4]. In this measurement, the magnetic field was parallel to the sample plane. Clear saturation and hysteresis are observed at both 7 and 300 K. This strongly indicates that the GaCrN layer is ferromagnetic at both temperatures. This observation is quite different from that for the recently reported GaMnN [8]. For GaMnN, paramagnetic properties are observed at low temperatures. For GaCrN, the saturation field was

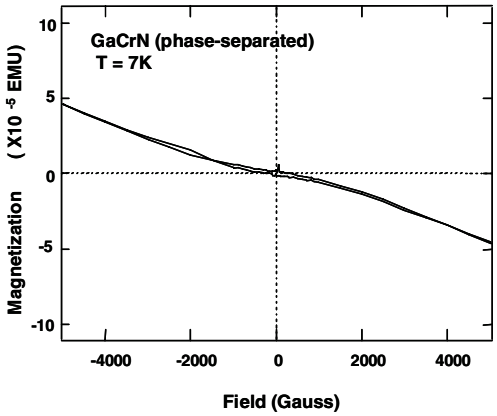

Figure 2. Dependence of magnetization on magnetic field at 7 K for GaCrN grown with Cr cell temperature of 940 °C (phase-separated sample).

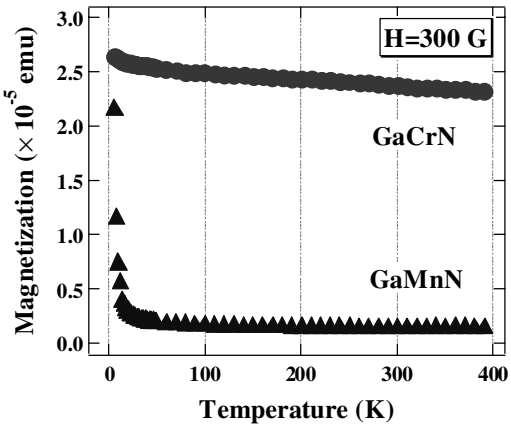

Figure 3. Temperature variation of magnetization for GaCrN and GaMnN. The rapid drop at low temperatures which indicates a paramagnetic component is not observed for GaCrN.

about 2 kOe and the coercivity H_c was about 55 Oe at 300 K. On the other hand, for the phase-separated sample grown with Cr cell temperature of 940 °C, ferromagnetic character was not observed even at 7 K, as shown in figure 2, where the contribution from the sapphire substrate is not extracted.

The magnetization versus temperature (M–T) curve for GaCrN is shown in figure 3 [4], where the M–T curve for a GaMnN sample grown by MBE with NH_3 as nitrogen source is also shown for comparison. A magnetic field of 300 G was applied parallel to the sample surface. The magnetization of GaCrN decreases very slowly with the increase of temperature and remains even at 400 K. This indicates that the Curie temperature of GaCrN exceeds at least 400 K. The Curie temperature for GaCrN could not be precisely determined in this study because of the operating-temperature limit of the SQUID equipment used.

As can be seen in figure 3, the magnetization for GaCrN decreases continuously with increasing temperature in the whole temperature range (from 7 to 400 K) and there is no discontinuous change in the curve.

For the GaMnN sample, the magnetization rapidly decreased with increasing the temperature from 7 to 50 K. The data shown here for GaMnN are very similar to those in [8].

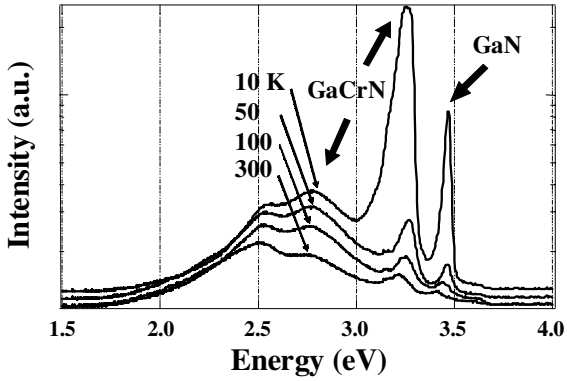

Figure 4. PL spectra for the GaCrN sample (Cr: 1.5%) as a function of temperature.

This behaviour suggests the existence of a paramagnetic phase in the GaMnN sample, which is consistent with the data for GaMnN grown by MBE with an RF-radical cell [9].

However, the paramagnetic component was not observed in the GaCrN magnetization curves. These results confirm that the observed ferromagnetism is attributed to the single magnetic phase in the GaCrN layer without any phase separation. In addition, as mentioned above, the XRD measurement showed the existence of single phase GaCrN without any other Cr-based compounds or alloys. Therefore, it is considered that the observed ferromagnetic behaviour in the magnetization curves is due to the existence of a new magnetic semiconductor, GaCrN, and that GaCrN is superior to GaMnN as a magnetic semiconductor.

2.3. Optical properties

Photoluminescence (PL) emission was observed from the grown GaCrN samples [5]. This is the first observation of PL emission from III–V-based magnetic semiconductors to the best of our knowledge. Figure 4 shows the temperature dependence of the PL spectrum for GaCrN with Cr concentration of 1.5%.

Two PL peaks at 3.47 and at 3.29 eV at 10 K are observed. It is considered that the PL peak at 3.47 eV is due to the free excitonic transition in hexagonal GaN and comes from the GaN buffer layer which is grown below the GaCrN layer (thickness $\sim$ 40 nm).

Stronger PL emission peaking at 3.29 eV comes from the GaCrN layer. This peak energy shifts to lower energy as the temperature increases, in a similar manner to that of the 3.47 eV peak. The integrated PL intensity of the GaCrN peak increased with the excitation power density and no saturation of the PL intensity was observed (not shown). Therefore, we conclude that the 3.29 eV peak, which is about 180 meV lower than that of the free excitonic transition in GaN, is attributed to the band-to-band transition in GaCrN. The origin of the 3.29 eV band is not clear at this stage. We consider that this band could be assigned to the p–d hybridized state, although further studies are needed.

These observations will provide novel functional devices that control charges (electrons and holes) and spins as well as photons.

3. GaGdN

GaGdN layers were grown on the (0001) Si face of 6H-SiC substrate by RF-MBE [10]. The layer structure was GaGdN(250 nm)/GaN(250 nm)/AlN(20 nm)/SiC. The Gd composition x was estimated to be about 0.06 by x-ray photoemission spectroscopy (XPS). X-ray diffraction

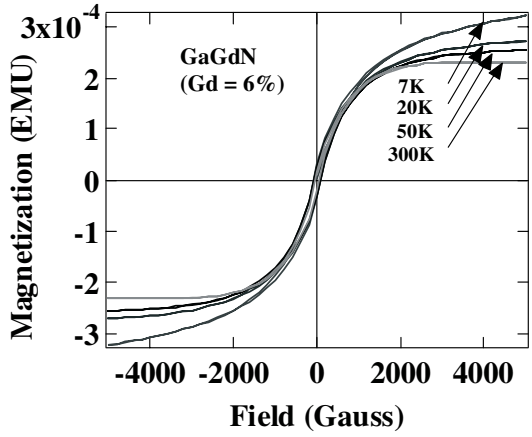

Figure 5. *M–H* curves for the GaGdN sample at 7–300 K.

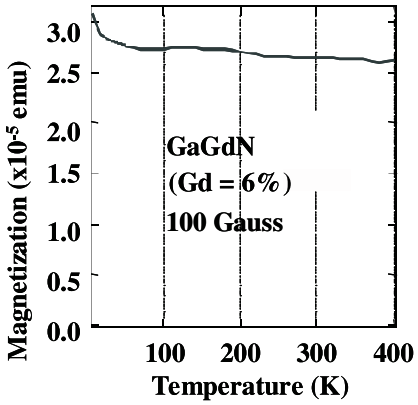

Figure 6. Temperature dependence of magnetization for the GaGdN sample at applied magnetic field of 100 G.

and EXAFS measurements showed no phase separation and that the Gd atoms occupy the Ga sites.

Figure 5 shows the *M–H* curves at 7–300 K [6]. The magnetic field was parallel to the sample plane. Hysteresis curves were observed at 7–300 K. This strongly indicates that the $Ga_{0.94}Gd_{0.06}N$ ternary layer is ferromagnetic at both temperatures. The saturation field was about 2 kG and the coercivity H_c was about 70 Oe at 300 K.

Figure 6 shows the temperature dependence of magnetization at an applied magnetic field of 100 G [6]. The magnetization decreased slowly with increasing temperature and remained even at 400 K. This indicates that the Curie temperature of the $Ga_{0.94}Gd_{0.06}N$ ternary layer is higher than 400 K. As can be seen in figure 6, the magnetization for the $Ga_{0.94}Gd_{0.06}N$ ternary layer decreased continuously with increasing temperature in the whole temperature range from 7 to 400 K, and there was no discontinuous change in the curve, though it is inferior to that for GaCrN. This result is very interesting because the rare-earth-doped GaN also showed ferromagnetism.

Figure 7 shows the PL spectrum for GaGdN at room temperature. A sharp PL emission peak was observed compared with the transition-metal-doped GaN, GaCrN. This peak may

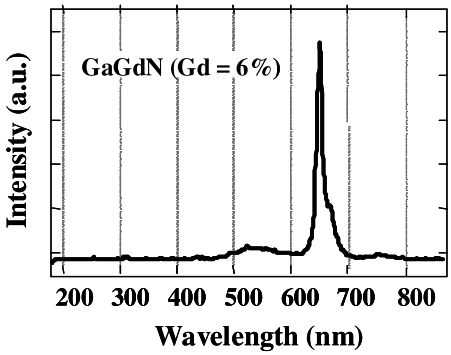

Figure 7. PL spectrum for the GaGdN sample at room temperature.

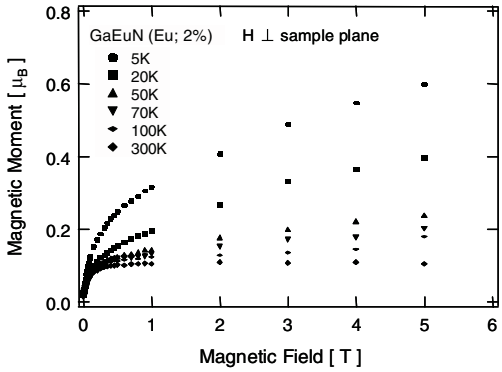

Figure 8. Magnetic field dependence of the magnetic moment per Eu ion in units of Bohr magneton for $Ga_{1-x}Eu_xN$ with $x = 0.02$. The external field was applied perpendicular to the sample plane.

come from the atomic level transition at rare-earth atoms. Therefore, we can consider different device applications from the transition-metal-doped GaN.

4. GaEuN

The GaEuN sample studied in this paper was grown by ammonia molecular beam epitaxy on an (0001) sapphire substrate. The details of the growth conditions have been reported elsewhere [11, 12]. After the sapphire substrate surface was nitrided, a low temperature GaN buffer layer was grown. On this buffer layer, an Eu-doped GaN layer was grown at 750 °C. The thickness of the $Ga_{1-x}Eu_xN$ layer was 0.8 μm and the Eu content x was 0.02. The photoluminescence (PL) spectra of GaEuN exhibit sharp luminescence due to the intra-atomic f–f transitions at 622 nm, attributable to the $^5D_0$–$^7F_2$ transition of Eu^{3+} [11, 12]. This indicates that the majority of Eu ions take a valence state of 3+ in GaN. The structural properties of GaEuN investigated by extended x-ray absorption fine structure (EXAFS) measurement showed that Eu ions are surrounded by nitrogen atoms with a coordination number of approximately 4 at their first-nearest neighbour, indicating the substitution of Eu ions into Ga lattice sites [13].

Figure 8 shows the magnetic field dependence of the magnetic moment per Eu ion in units of Bohr magneton for $Ga_{0.98}Eu_{0.02}N$ in the 0 to 5.0 T magnetic field range [7]. The external field was applied perpendicular to the sample plane. As can be seen in figure 8, at high temperatures

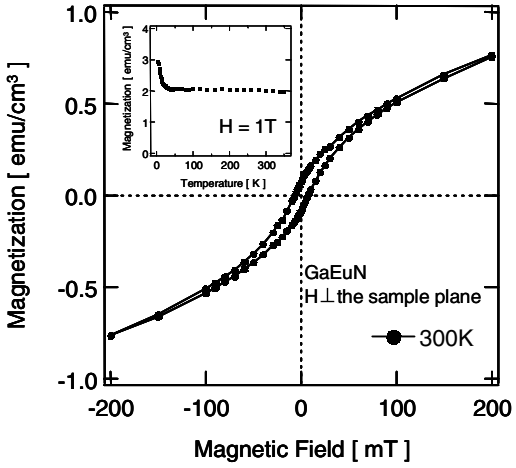

Figure 9. The external field dependence of the magnetization in a small magnetic field range at 300 K; the inset shows the magnetization versus temperature (M–T) curve. An external magnetic field of 1.0 T was applied perpendicular to the sample plane during the M–T measurement.

the magnetic moment saturates at approximately 0.5 T, while at low temperatures the magnetic moment gradually saturates with increasing magnetic field, which is quite different from that expected from the nonmagnetic F_0 ground level of Eu^{3+} ions, indicating the coexistence of two phases, a ferromagnetic-like phase and a paramagnetic-like phase.

Figure 9 shows the magnetic field dependence of the magnetization in a small magnetic field range at 300 K, and the inset shows the magnetization versus temperature (M–T) curve [7]. An external magnetic field of 1 T was applied perpendicular to the sample plane during the M–T measurement. A hysteresis loop is seen in figure 9, indicating the existence of a ferromagnetic-like phase. The Curie temperature (T_C) was above room temperature, as can be seen in the M–T curve in the inset of figure 9.

We attempted to explain the experimental results theoretically by introducing a c-axis-oriented molecular-field term that acts as an RKKY-type interaction via the spin-polarized valence-band of GaN [7]. A detailed description is reported in [7]. In this paper, we will describe it briefly. Figure 10 shows an example of the theoretical calculation results. The saturation dependences in the M–H curves are observed. We conclude that Eu ions interact with other Eu ions through an RKKY-type interaction. However, the temperature dependence of the calculated magnetic moment differs somewhat from the experimental results. The calculated magnetic moments at 5–70 K are nearly independent of temperature and decrease markedly from 100 to 300 K, while the experimental results show a significant decrease in magnetic moment at 5–70 K and a slow decrease at 100–300 K. The origin of the difference between the experimental results and the calculated results is not completely clear at present. We consider that this disagreement is caused by the coexistence of divalent and trivalent Eu ions and the interaction between them. The coexistence of divalent and trivalent Eu ions was confirmed by the observation of the structures from the divalent and trivalent Eu ions in the x-ray absorption near-edge structure (XANES) spectrum for the GaEuN sample [14].

5. Summary

We have grown new III–V-based magnetic semiconductors and studied their physical properties. For the transition-metal-doped GaN, GaCrN, high temperature (>400 K)

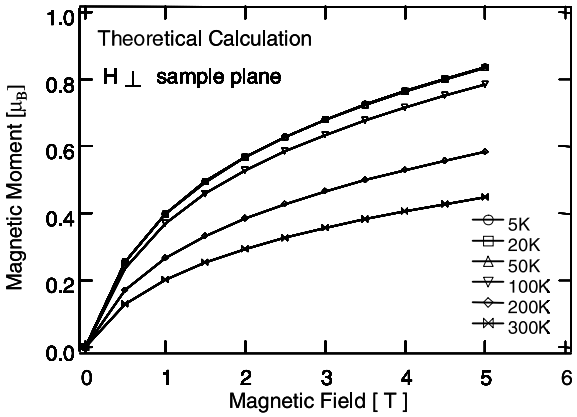

Figure 10. Magnetic field dependence of the theoretically calculated magnetic moment per Eu ion for temperatures $T = 5$, 20, 50, 100, 200 and 300 K with molecular-field term. The magnetic field is perpendicular to the sample plane.

ferromagnetism and PL emission were observed. Clear saturation and hysteresis were observed at all measuring temperatures. For the rare-earth-doped GaN, GaGdN and GaEuN, we also observed a similar ferromagnetism. Novel functional devices that control charges (electrons, holes), and spins as well as photons, such as spin tunnel devices, circular polarization light emitting devices, are considered candidates to be fabricated by using these magnetic semiconductors.

Acknowledgments

This work was supported by the Ministry of Education, Culture, Sports, Science and Technology (MEXT) of Japan through MEXT special coordination Funds for Promoting Science and Technology (Nanospintronics Design and Realization, NDR) and in part by the Grant-in-Aid for Specially Promoted Research and the 21st COE Program from the MEXT of Japan.

References

[1] Munekata H, Ohno H, von Molnar S, Segmuelier A, Chang L L and Esaka L 1989 *Phys. Rev. Lett.* **63** 1849
[2] Ohno H, Shen A, Matsukura F, Oiwa A, Endo A, Katsumoto S and Iye Y 1996 *Appl. Phys. Lett.* **69** 363
[3] Sato K and Katayama-Yoshida H 2001 *Japan. J. Appl. Phys.* **40** L485
[4] Hashimoto M, Zhou Y K, Kanamura M and Asahi H 2002 *Solid State Commun.* **122** 37
[5] Hashimoto M, Zhou Y K, Kanamura M, Katayama-Yoshida H and Asahi H 2003 *J. Cryst. Growth* **251** 327
[6] Teraguchi N, Suzuki A, Nanishi Y, Zhou Y K, Hashimoto M and Asahi H 2002 *Solid State Commun.* **122** 651
[7] Hashimoto M, Yanase A, Asano R, Tanaka H, Bang H, Akimoto K and Asahi H 2003 *Japan. J. Appl. Phys.* **42** L1112
[8] Sonoda S, Shimizu S, Sasaki T, Yamamoto Y and Hori H 2002 *J. Cryst. Growth* **237/239** 1358
[9] Kondo T, Kuwabara S, Oiwa H and Munekata H 2002 *J. Cryst. Growth* **237/239** 1353
[10] Teraguchi N, Suzuki A, Saito Y, Yamaguchi T, Araki T and Nanishi Y 2001 *J. Cryst. Growth* **230** 392
[11] Morishima S, Maruyama T and Akimoto K 2000 *J. Cryst. Growth* **209** 378
[12] Morishima S, Maruyama T, Tanaka M, Matsumoto Y and Akimoto K 1999 *Phys. Status Solidi* a **176** 113
[13] Bang H, Morishima S, Li Z, Akimoto K, Nomura M and Yagi E 2002 *J. Cryst. Growth* **237/239** 1027
[14] Tanaka H, Hashimoto M, Emura S, Yanase A, Asano R, Zhou Y K, Bang H, Akimoto K, Honma T, Umesaki N and Asahi H 2003 *Phys. Status Solidi* c **0** 2864